

Large-Angle Rigid Body Dynamics of a Floating Offshore Wind Turbine using Euler's Equations of Motion

Bert Sweetman
Texas A&M University

Lei Wang
Texas A&M University

Abstract: Floating structures have been proposed to support offshore wind turbines in deep water, where environmental forcing could subject the rotor to meaningful angular displacements in both precession and nutation, offering design challenges beyond conventional bottom-founded structures. This paper offers theoretical developments underlying an efficient methodology to compute large-angle rigid body rotations of a floating wind turbine in the time domain. One set of Euler angles is introduced to describe spatial rotations of a combined tower-RNA (rotor nacelle assembly) as a single rigid body; necessary transformations are developed to enable inclusion of structural motions in computation of environmental loading. A worked example of a floating wind turbine subject to wind and waves is presented. More recent work has built upon this work by applying a second set of Euler angles to describe motion of the RNA to assess the dynamic effects of the spinning rotor; present initiatives are to expand the method to the general motion of n rigid bodies.

1. Introduction and Background: Environmental, aesthetic and political pressures continue to push for siting offshore wind turbines beyond sight of land, where waters tend to be deeper, and use of floating structures is likely to be considered. Highly compliant floating support structures allowing large angular displacements are likely to be very cost-competitive for deep water. These floating towers, or very tall flexible ones, will be more compliant to wind and waves, making computation of structural dynamics both more challenging and more important to the design process. This paper offers a theoretical basis for calculation of large angular displacements of floating wind turbines. Three Euler angles associated with tower motion are used to establish the Euler dynamics equations, in which the order of the angular rotations are explicitly considered. In addition

to accurate computation of large-angle displacements, Euler's rotational coordinate system enables considerable engineering insight into rotational dynamics, and can enable rotational inertia to be uncoupled from translational. For these reasons, the Euler dynamic equations have been widely applied to rotational bodies, including attitude motion of space vehicle (e.g. [1]) and rolling motion of the ship (e.g. [2]).

The five main contributions of this paper are: 1) application of the Euler dynamic equations to compute dynamic motions of a floating wind turbine, 2) application of a 3-1-3 sequence form of the Euler dynamic equations that separates rotation of the body from rotation of the coordinate system to simplify derivations and improve efficiency, 3) selection of a translating-rotating coordinate system originating at the center of mass to simplify and uncouple the equations of motion, 4) development of the transformation matrices described by Euler angles between a rotating Cartesian coordinate system, in which it is convenient to compute dynamic motion, and a translating Cartesian system, in which it is convenient to compute environmental forcing, and 5) a simplification of the dynamic equations to only the two rotational degrees of freedom most important to floating turbines. The overall result is that time-domain simulations can be completed more accurately than through use of typical multi-DOF methods that assume small-angle rotations, and these simulations can be computed using significantly less computational power. An example is presented in which the new method has been implemented in MATLAB and applied to a hypothetical TLP-based floating wind turbine. A free-vibration case illustrates numerical stability and the numerical conservation of energy. A more realistic case includes structural response to wind and wave forcing; results of the simplified 2-D method are critically compared to those resulting

from solution of the complete 3-DOF system.

Perhaps the most significant existing computational tool for simulating the dynamic behavior of floating offshore wind turbines is the NREL FAST computer program [3]. FAST is a comprehensive aero-elastic simulator for which recent developments enable hydrodynamic transfer functions computed using an existing code (WAMIT) [4] to be applied with irregular seas to predict overall floating wind turbine response. The work presented here is fundamentally different from the core of the NREL FAST model. FAST solves the dynamic equations of motion in a conventional way in which the order of the angles of rotation is not considered. This method results in a non-orthonormal transformation matrix between Cartesian coordinate systems, which is made mathematically orthonormal by the Frobenius norm. The Frobenius norm enables FAST to have reasonable accuracy for angular motions up to around 20 degrees [5]. The new methodology presented here enables solution of the non-linear rotational equations of motion for large-amplitude motion of a rigid body. No mathematical correction is needed because sequenced Euler angles are used directly throughout development and solution of the equations of motion.

In other work relevant to floating wind turbines, Nielsen et al. (2006) [6] applied experimental and numerical simulation to investigate pitch and surge responses of a spar-type floating offshore wind turbine subject to both wind and wave forcing in the frequency domain. The kinematic model of the turbine included the effect of gyro moments associated with precession and nutation, but the underlying theory is applicable to only small-angles. Shim et al. (2006) [7] developed a numerical time-domain model for fully coupled dynamic analysis of a floating wind turbine. FAST was used to demonstrate the nonlinearity of both structural motions and external forcing, including the blade-rotor dynamics, mooring dynamics, and platform motion. Small angle theory was also applied in that work.

The work presented here differs from prior work in that here the complete rotational dynamics problem is developed and solved in terms of Euler angles, explicitly considering the order of angular rotations. The first critical step in rigorous treatment of the dynamic system is development of optimal coordinate systems.

2. Coordinate Systems: Coordinate systems (X, Y, Z) and (x, y, z) both originate at the center of mass of the moving body (Fig. 1). The (X, Y, Z) system is non-rotating, while (x, y, z) rotates with the

z -axis remaining fixed at the centerline of the moving tower. Angular differences between these coordinate systems define a set of independent Euler angles, $(\theta_1, \theta_2, \eta)$. The angle θ_1 lies between the vertical Z , and the tower centerline, z , with positive rotations right-handed about the positive x -axis. Angle θ_2 lies between Y and y_p with positive right-handed along positive Z ; y_p is the projection of y on the horizontal X - Y plane, and opposite to the projection of z onto X - Y . The first two Euler angles, θ_1 and θ_2 , fully define the location of the (x, y, z) coordinate system. The third Euler angle, η , describes a rotation about the moving z -axis, with positive rotations being right-handed about positive z . This third Euler angle is mathematically defined, and does not describe a measurable position of the moving tower. Euler velocity, $\dot{\eta}$, is necessary to describe the absolute velocity of the tower, and $\ddot{\eta}$ enables the sum of the accelerations around the z -axis to sum to the total acceleration of the body in space (Eqn. (11), later). A fourth angle, θ_3 , describes physical rotation of the tower about its own centerline; θ_3 is a function of the three Euler angles, but is not an Euler angle itself.

For large angular displacements in space, the order in which the angles of rotation are applied is important; there are twelve possible Euler angles sequences. Here, a 3-1-3 sequence is used to describe the position of the rotating tower (e.g., [8]). The three rotational axes are x , y and z , so a 3-1-3 sequence indicates the Euler sequence is z - x - z , or in detail: 1) first, rotate the upright tower about the z -axis (then coincident with Z) through an angle θ_2 measured in the horizontal plane XOY ; 2) next, rotate the resultant tower about the resulting x -axis through an angle θ_1 measured in the vertical plane ZOy_p , and 3) finally, rotate the tower about the new z -axis (not coincident with Z for non-zero θ_1) through the third Euler angle, η . The Euler equations of motion are derived and solved in terms of θ_2 , θ_1 , and η in the 3-1-3 sequence. This combination enables considerable simplification in the derivation of Euler's kinematic equations, which in turn results in dramatically simpler equations of motion, and improved numerical efficiency.

3. Precession and Nutation: The rotor nacelle assembly (RNA) is rigidly mounted to the tower in this single-body problem. However, it is necessary to describe the motion of the RNA because the wind force is a function of precession angle, ϕ , and nutation angle, θ . Precession describes the horizontal orientation of the RNA, and is the angle between the Y - and B_p -axes, positive around the positive Z -axis; B_p is the projection of spin axis, B , on the horizon-

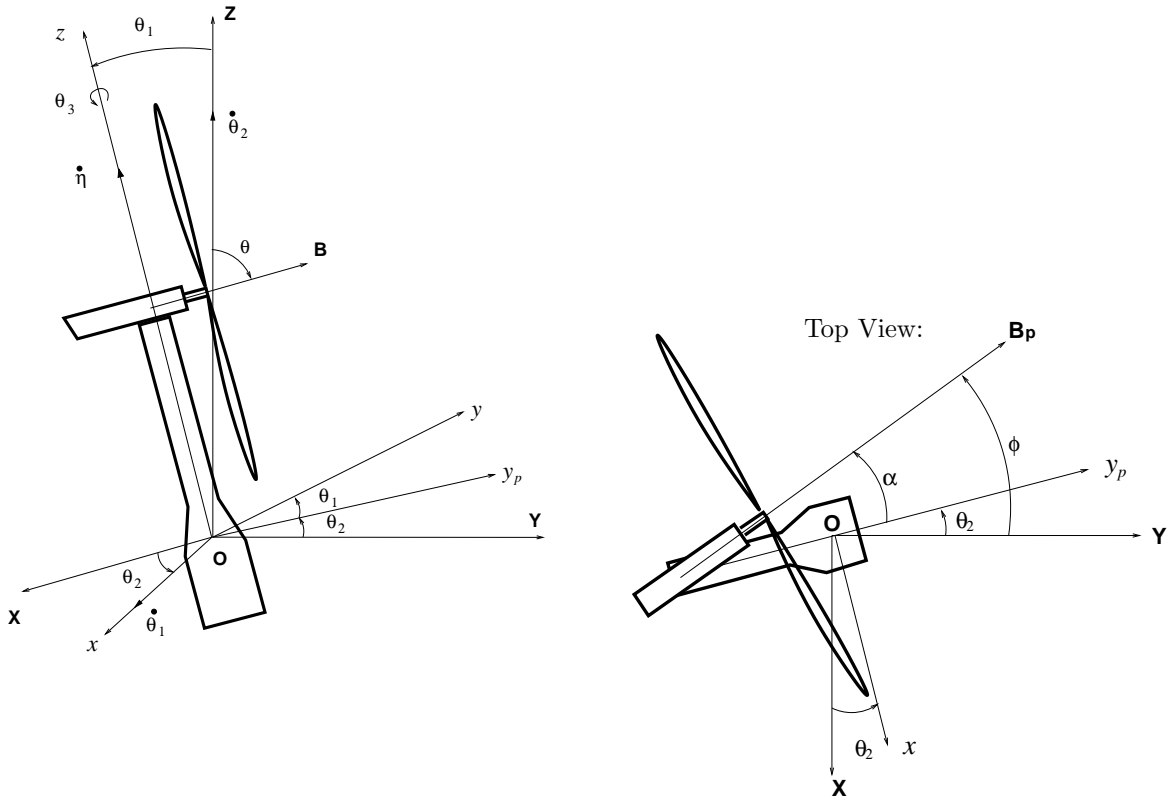


Figure 1: Coordinate systems (X, Y, Z) and (x, y, z)

tal plane. Precession is generally a function of both nacelle yaw and tower motion, but for wind force calculations, tower motion effects on ϕ can reasonably be neglected.

Nutation describes the orientation of the RNA from horizontal. Nutation angle, θ , is measured from the Z -axis to the B -axis, with $\theta = -\pi/2$ defining a horizontal B -axis. The angle α is the difference between the y_p -axis and B_p , the projection of the spin axis onto the horizontal: $\alpha = \phi - \theta_2$, with positive in the same direction as ϕ . The combination of angles ϕ and θ indicates the difference between the wind direction and the orientation of the moving spin axis.

Trigonometric expressions for the nutation angle can be obtained by geometrical insight (Fig. 2). Perspective is improved by temporarily rotating the (x, y, z) coordinate system such that the x -axis is vertical. Clarity of perspective is improved by showing both θ_1 and α with negative values, which has no influence on the geometrical derivation. Also, the B -axis is translated to OB . Here, x -, B - and y -axes are coplanar. OB_p is the intersection line between the planes xOy_p and ZOB . An additional plane abc is constructed parallel to the plane yOz . Thus, the line ab is parallel to the Z -axis, ac parallel to the y -axis, and bc parallel to the y_p -axis, which implies $Ob \perp ab$, $bc \perp ab$, $Oc \perp bc$ and $\angle acb = \theta_1$.

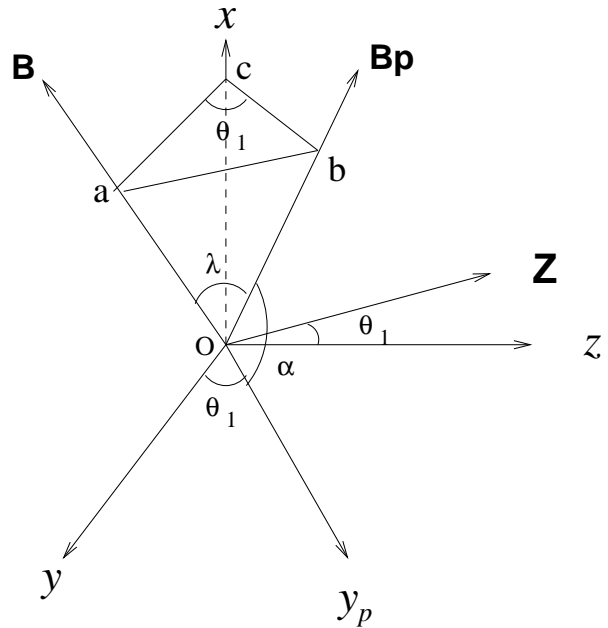


Figure 2: Rotated (x, y, z) coordinate system for derivation of nutation angle, θ

The angle λ is defined as the difference between the B_p - and B -axes in Fig. 2. Setting $Oa = 1$ in the right triangle abO results in $Ob = \cos \lambda$, $ab = \sin \lambda$

and thus in the right triangle abc , $bc = \sin \lambda / \tan \theta_1$. Then in the right triangle Ocb , $\sin(\frac{\pi}{2} - \alpha) = bc/Ob$, such that $\lambda = \arctan(\tan \theta_1 \cos \alpha)$:

$$\theta = -\frac{\pi}{2} + \lambda \quad (1)$$

$$\theta = -\frac{\pi}{2} + \arctan(\tan \theta_1 \cos \alpha) \quad (2)$$

4. Rotational Motion of the Combined Tower and RNA: Beginning at first principles, the sum of the moments resulting from externally applied forces about the center of mass of a body in a translating-rotating system, (x, y, z) , equals the change of the momentum within the coordinate system plus that associated with the movement of the coordinate system (e.g. [8]):

$$\sum \vec{M} = \dot{\vec{H}}_O = (\dot{\vec{H}}_O)_{xyz} + \vec{\Omega} \times \vec{H}_O \quad (3)$$

Vector $\vec{\Omega}$ describes the angular velocity of (x, y, z) with respect to (X, Y, Z) . The x -, y - and z -axes are chosen as the principal axes of the body, so the products of inertia in \vec{H}_O disappear, and locating the coordinate system at the center of mass decouples the rotational and translational degrees of freedom. For this work, this decoupling enables solution of the rotational degrees of freedom without regard for the translational; alternatively, it would also be straightforward to include these independent translational DOF's if needed. Following e.g. Hibbeler [8], Eqn. (3) expands to three scalar equations:

$$\sum M_x = I_x \dot{\omega}_x - I_y \omega_y \Omega_z + I_z \omega_z \Omega_y \quad (4)$$

$$\sum M_y = I_y \dot{\omega}_y - I_z \omega_z \Omega_x + I_x \omega_x \Omega_z \quad (5)$$

$$\sum M_z = I_z \dot{\omega}_z - I_x \omega_x \Omega_y + I_y \omega_y \Omega_x \quad (6)$$

where $\vec{\omega}$ describes the rotation of the tower in space. The more conventional form of Eqns (4)–(6) has $\vec{\omega} = \vec{\Omega}$, such that the coordinate system is fixed to the body. The difference between motion of the (x, y, z) coordinate system, $\vec{\Omega}$, and that of the body, $\vec{\omega}$, is the Euler angle η : $\vec{\omega} = \vec{\Omega} + \eta \vec{k}$. The associated Euler kinematic equations are:

$$\vec{\omega} = \omega_x \vec{i} + \omega_y \vec{j} + \omega_z \vec{k} \quad (7)$$

$$= \dot{\theta}_1 \vec{i} + (\dot{\theta}_2 \sin \theta_1) \vec{j} + (\dot{\theta}_2 \cos \theta_1 + \dot{\eta}) \vec{k} \quad (8)$$

Continuing to follow e.g. [8], component-wise expressions for ω , $\dot{\omega}$ and Ω are substituted into a component-wise expansion of Eqn. (3). Here, the RNA is treated as a point-mass centered on top of

the symmetrical tower such that $I_x = I_y = I$. The resulting Euler dynamic equations are:

$$\sum M_x = I(\ddot{\theta}_1 - \dot{\theta}_2^2 \sin \theta_1 \cos \theta_1) + I_z \dot{\theta}_2 \sin \theta_1 (\dot{\theta}_2 \cos \theta_1 + \dot{\eta}) \quad (9)$$

$$\sum M_y = I(\ddot{\theta}_2 \sin \theta_1 + 2\dot{\theta}_1 \dot{\theta}_2 \cos \theta_1) - I_z \dot{\theta}_1 (\dot{\theta}_2 \cos \theta_1 + \dot{\eta}) \quad (10)$$

$$\sum M_z = I_z(\ddot{\eta} + \ddot{\theta}_2 \cos \theta_1 - \dot{\theta}_1 \dot{\theta}_2 \sin \theta_1) \quad (11)$$

The moments on the left hand side of Eqns. (9)–(11) are externally applied about the mass center of the body:

$$\sum M_x = M_{windx} + M_{wavex} - M_{\theta_1} \quad (12)$$

$$\sum M_y = M_{windy} + M_{wavey} \quad (13)$$

$$\sum M_z = M_{windz} + M_{wavez} - M_{\theta_3} \quad (14)$$

where environmental forcing M_{wind} and M_{wave} are decomposed to x -, y - and z -directions; M_{θ_1} and M_{θ_3} represent the restoring moments and are along the positive directions of x - and z -axes, respectively. In some applications it may be convenient to express the torsional restoring moment of the vertical mooring system projected onto the z -axis as $M_{\theta_3} = K_Z \theta_Z \cos \theta_1$. The twist of the mooring system, θ_Z , is obtained by integrating $\dot{\theta}_Z$, which is found by projecting the Euler angular velocities onto the Z -axis:

$$\dot{\theta}_Z = \dot{\theta}_2 + \dot{\eta} \cos \theta_1 \quad (15)$$

5. Reduction to a 2-DOF System: The absolute angular velocity and acceleration of the tower rotation about the z -axis are the \vec{k} -direction components of Eqn. (8) and its derivative:

$$\dot{\theta}_3 = \dot{\eta} + \dot{\theta}_2 \cos \theta_1 \quad (16)$$

$$\ddot{\theta}_3 = \ddot{\eta} + \ddot{\theta}_2 \cos \theta_1 - \dot{\theta}_1 \dot{\theta}_2 \sin \theta_1 \quad (17)$$

Substituting Eqns. (16) and (17) into Eqns. (9)–(11) results in equations of motion in terms of three physical degrees of freedom $(\theta_1, \theta_2, \theta_3)$:

$$\sum M_x = I(\ddot{\theta}_1 - \dot{\theta}_2^2 \sin \theta_1 \cos \theta_1) + I_z \dot{\theta}_2 \sin \theta_1 \dot{\theta}_3 \quad (18)$$

$$\sum M_y = I(\ddot{\theta}_2 \sin \theta_1 + 2\dot{\theta}_1 \dot{\theta}_2 \cos \theta_1) - I_z \dot{\theta}_1 \dot{\theta}_3 \quad (19)$$

$$\sum M_z = I_z \ddot{\theta}_3 \quad (20)$$

Solution of these equations as equations of motion is impractical because the variable θ_3 is not independent of θ_1 and θ_2 . However, for some applications,

θ_3 may be unimportant. Tall, slender towers have θ_1 and θ_2 as the dominant degrees of freedom because they have both larger excursions and larger moments of inertia. Assuming the moment of inertia about the centerline of the tower, I_z , is much smaller than those in the θ_1 - and θ_2 -directions, i.e., $I_z \approx 0$:

$$\sum M_x = I(\ddot{\theta}_1 - \dot{\theta}_2^2 \sin \theta_1 \cos \theta_1) \quad (21)$$

$$\sum M_y = I(\ddot{\theta}_2 \sin \theta_1 + 2\dot{\theta}_1 \dot{\theta}_2 \cos \theta_1) \quad (22)$$

$$\sum M_z = 0 \quad (23)$$

which reduces the equations of motion to only 2 independent Euler Angles. The effects of this simplification are assessed through critical comparison in the Example section of this paper.

6. Transformations for Wind Forcing: The environmental forcing in Eqns. (12)-(14) can be computed considering both the wind and waves acting on the structure, and the relative motion of the tower through the air and water. To obtain wind forcing in terms of the (x, y, z) coordinate system, the wind forces are first calculated in (X, Y, Z) and then decomposed onto (x, y, z) which are finally used to compute the moments. The linear velocity of the RNA through the air is computed from the angular velocities:

$$\vec{v}_{\theta_1} = \dot{\theta}_1 \times \vec{r} = \dot{\theta}_1 l \quad (24)$$

$$\vec{v}_{\theta_2} = \dot{\theta}_2 \times \vec{r} = \dot{\theta}_2 l \sin \theta_1 \quad (25)$$

where \vec{v}_{θ_1} and \vec{v}_{θ_2} are linear-velocity components at a location along the z -axis (here, the RNA); angular velocity $\dot{\theta}_1$ is along the negative direction of the y -axis and $\dot{\theta}_2$ is along the positive direction of the x -axis. Vector \vec{r} is the radius from O to that location, and l is the magnitude of \vec{r} .

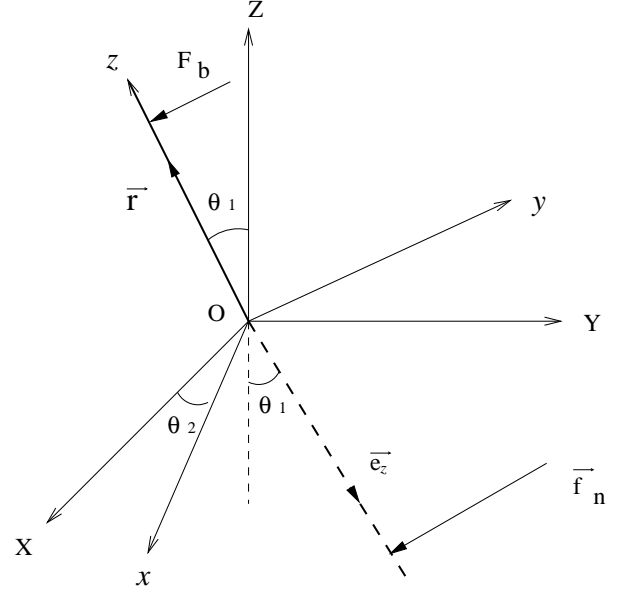


Figure 3: Coordinate system for derivation of environmental forcing

An expression for the velocity of the wind relative to the RNA, V_{rb} , along the negative B -axis, can be developed from Eqns. (24) and (25) and direction cosines, which can be derived geometrically or through use of transformation matrices (Part 2 of this series):

$$\vec{V}_{rb} = \vec{v}_w + \vec{v}_{\theta_1}(-\cos \angle BOy) + \vec{v}_{\theta_2} \cos \angle BOx \quad (26)$$

$$V_{rb} = -v_w + \dot{\theta}_1 l (\cos \theta_1 \sin \theta \cos \alpha - \cos \theta \sin \theta_1) + \dot{\theta}_2 l \sin \theta_1 \sin \theta \sin \alpha \quad (27)$$

where $v_w = |\vec{v}_w|$ and is along the negative B -axis. The resulting relative velocity can be used to compute the wind forces acting on the RNA in the (X, Y, Z) coordinate system, after which they must be transformed into the (x, y, z) system for application in the equations of motion. Decomposing the thrust force, F_b , onto the (x, y, z) system, calculating moments as a cross product expressed as a cofactor expansion, and finally substituting Eqn. (2):

$$\vec{M}_{wind} = \vec{r} \times \vec{F}_b = \quad (28)$$

$$\begin{bmatrix} \vec{i} & \vec{j} & \vec{k} \\ 0 & 0 & l \\ -F_b \cos \angle BOx & -F_b \cos \angle BOy & -F_b \cos \angle BOz \end{bmatrix}$$

$$\begin{aligned} M_{windx} &= F_b l \cos \angle BOy \\ &= F_b l (\cos \theta \sin \theta_1 - \cos \theta_1 \sin \theta \cos \alpha) \end{aligned}$$

$$= F_b l \frac{\cos \alpha}{\sqrt{\cos^2 \alpha + \cos^2 \theta_1 \sin^2 \alpha}} \quad (29)$$

$$M_{windy} = -F_b l \cos \angle BOx = -F_b l \sin \theta \sin \alpha$$

$$= F_b l \frac{\cos \theta_1 \sin \alpha}{\sqrt{\cos^2 \alpha + \cos^2 \theta_1 \sin^2 \alpha}} \quad (30)$$

$$M_{windz} = 0 \quad (31)$$

7. Transformations for Wave Forcing: Similar to the calculation of wind forcing, wave forces are computed in the (X, Y, Z) coordinate system, decomposed into the (x, y, z) system, and used to compute the moments. Waves are assumed to progress down the negative Y -axis. The wave kinematic velocity relative to the moving tower is \vec{V}_{rt} . Determination of \vec{V}_{rt} requires expression of velocity vectors for both the tower and the wave kinematics normal to the axis of the tower in the (X, Y, Z) coordinate system. In general, 3-D rotation matrices of a regular right-handed (x_1, x_2, x_3) coordinate system can be expressed as e.g. [9]:

$$T_{x_1}(\beta) = \begin{bmatrix} 1 & 0 & 0 \\ 0 & \cos \beta & -\sin \beta \\ 0 & \sin \beta & \cos \beta \end{bmatrix} \quad (32)$$

$$T_{x_2}(\beta) = \begin{bmatrix} \cos \beta & 0 & \sin \beta \\ 0 & 1 & 0 \\ -\sin \beta & 0 & \cos \beta \end{bmatrix} \quad (33)$$

$$T_{x_3}(\beta) = \begin{bmatrix} \cos \beta & -\sin \beta & 0 \\ \sin \beta & \cos \beta & 0 \\ 0 & 0 & 1 \end{bmatrix} \quad (34)$$

where, e.g., $T_{x_1}(\beta)$ indicates rotating some arbitrary angle, β , about the x_1 -axis. The 3-1-3 transformation matrix from a body-fixed coordinate system to an inertial coordinate system through arbitrary angles α , β and γ can generally be expressed as $T = T_{x_3}(\alpha)T_{x_1}(\beta)T_{x_3}(\gamma)$. Here, the location of the centerline of the tower is fully defined by (θ_1, θ_2) , with the final rotation about the z -axis being irrelevant, so the transformation matrix from (x, y, z) to (X, Y, Z) can be computed from the general form:

$$T_{x_3}(\theta_2)T_{x_1}(\theta_1) = \begin{bmatrix} \cos \angle XOx & \cos \angle XOy & \cos \angle XOz \\ \cos \angle YOx & \cos \angle YOy & \cos \angle YOz \\ \cos \angle ZOx & \cos \angle ZOy & \cos \angle ZOz \end{bmatrix} \quad (35)$$

$$T_Z(\theta_2)T_x(\theta_1) =$$

$$= \begin{bmatrix} \cos \theta_2 & -\cos \theta_1 \sin \theta_2 & \sin \theta_1 \sin \theta_2 \\ \sin \theta_2 & \cos \theta_1 \cos \theta_2 & -\cos \theta_2 \sin \theta_1 \\ 0 & \sin \theta_1 & \cos \theta_1 \end{bmatrix} \quad (36)$$

The instantaneous unit vector along the negative z -axis can be deduced directly from Fig. 3:

$$\vec{e}_z = -\cos \angle XOz \vec{i}_I - \cos \angle YOz \vec{j}_I - \cos \angle ZOz \vec{k}_I \quad (37)$$

where \vec{i}_I , \vec{j}_I and \vec{k}_I are unit vectors in the X -, Y - and Z -directions, and the direction cosines appear as matrix elements in Equation 36. The unit vector \vec{e}_z can then be used to find the relative normal velocity:

$$\vec{V}_{rt} = \vec{e}_z \times (\vec{V}_r \times \vec{e}_z) \quad (38)$$

where \vec{V}_r is the relative velocity of the wave to the submerged tower: $\vec{V}_r = \vec{V} - \vec{V}_t$, in which $\vec{V} = (0, u_Y, u_Z)$ is the wave kinematic velocity in the YOZ plane.

The transformation matrix, Eqn. (36), is again used to compute the structural velocity, \vec{V}_t . Linear velocities \vec{v}_{θ_1} and \vec{v}_{θ_2} , are found as in Eqns. (24) and (25), but with \vec{r} now along the negative direction of the z -axis for the submerged tower, such that angular velocity \vec{v}_{θ_1} is along the positive direction of the y -axis and \vec{v}_{θ_2} is along the negative direction of the x -axis. Decomposing the linear velocities into the (X, Y, Z) system:

$$\begin{aligned} \vec{V}_t &= \vec{v}_{\theta_1, XYZ} + \vec{v}_{\theta_2, XYZ} \quad (39) \\ &= (\vec{v}_{\theta_1} \cos \angle XOy - \vec{v}_{\theta_2} \cos \angle XOx) \vec{i} + \\ &\quad (\vec{v}_{\theta_1} \cos \angle YOy - \vec{v}_{\theta_2} \cos \angle YOx) \vec{j} + \\ &\quad (\vec{v}_{\theta_1} \cos \angle ZOy - \vec{v}_{\theta_2} \cos \angle ZOx) \vec{k} \quad (40) \end{aligned}$$

It may also be useful to know the absolute kinematic wave-particle acceleration in absence of tower motion, \vec{V}_n . Similar to Eqn. (38), the normal component of wave acceleration, $\dot{\vec{V}}_n$, can be expressed as:

$$\dot{\vec{V}}_n = \vec{e}_z \times (\dot{\vec{V}} \times \vec{e}_z) \quad (41)$$

where $\dot{\vec{V}} = (0, u_Y, u_Z)$ is the wave acceleration vector in the YOZ plane.

Wave moments in the (x, y, z) coordinate system necessary for application in the Euler equations of motion can be computed using the relative velocities and accelerations resulting from Eqns. (38) and (41) at finite slices of the cylinder, then transforming the resulting forces into the (x, y, z) system (Eqn. (36)) and numerically integrating over the submerged length of the tower:

$$\vec{f}_{n,xyz} = [T_Z(\theta_2)T_x(\theta_1)]^{-1} \vec{f}_n \quad (42)$$

$$\vec{M}_{wave} = \int_r (\vec{r} \times \vec{f}_{n,xyz}) dr \quad (43)$$

$$\vec{M}_{wave} = M_{wave_x} \vec{i} + M_{wave_y} \vec{j} + M_{wave_z} \vec{k} \quad (44)$$

where M_{wave_x} , M_{wave_y} and M_{wave_z} are three components of the moments of wave forces in the (x, y, z) coordinate system. In practice, the integral in Eqn. (43) is computed as a finite sum. Use of relative velocities in computation of wave forcing introduces damping in the θ_1 - and θ_2 -directions. Any damping in the θ_3 -direction can be added directly to the L.H.S. of Eqn. (14).

8. Example: The new methodologies are applied to a TLP-based floating wind turbine to compute angular motions in the time domain. Both the 3-D rotational equations (9)-(11) and the simplified 2-D equations (21)-(22) have been implemented in a MATLAB code that solves the equations of motion in the time domain using an existing ordinary differential equation solver (ODE45). Results are presented for three cases: 1) a free-vibration case, in absence of wind, wave, or damping to verify physically realistic behavior and that the equations of motion conserve energy, 2) a forced-vibration case that includes excitation by steady wind and regular sinusoidal waves for the complete 3-D rotational equations of motion, and finally 3) the same forced vibration case, but the simplified 2-D equations of motion are applied. Results of the 3-D and 2-D equations of motion are critically compared for this example structure.

Physical properties of the RNA including inertial moments are taken from a study of a 5MW offshore wind turbine [10]. Dimensions and inertial properties of the tower and the mooring system (Figure 4) are taken from an undergraduate student design project at Texas A&M University [11] because no full-scale TLP-based floating turbines have yet been built. The mass moment of inertia of the tower, $I = I_x = I_y$, is 9.155E9kg·m². The restoring moment in the θ_1 -direction is taken as $M_{\theta_1} = K_{\theta_1} \theta_1$. Stiffness K_{θ_1} varies from 0.25E10 N-m/rad for a vertical tower to 3.5E10 N-m/rad at $\theta_1 = 1.5$ rad and includes both hydrostatic stiffness and mechanical stiffness of the mooring system. Any gyroscopic effects of the spinning rotor are neglected. All simulations begin with initial conditions: $\theta_1 = \theta_2 = 0.5$ rad, $\eta = 0$ rad, $\dot{\theta}_1 = \dot{\theta}_2 = \dot{\eta} = 0.05$ rad/s, and $\phi = 0.5$ rad.

The environmental conditions for the forced cases are: wind speed at hub height: 18.2 m/s, peak-to-trough wave height: 5.0 m, wave period: 11.2 seconds. Wind force computations include motion of the rotor through the air, but the horizontal project of the spin axis is assumed to point directly into

the wind, regardless of tower motion. Water particle kinematics are evaluated using linear wave theory.

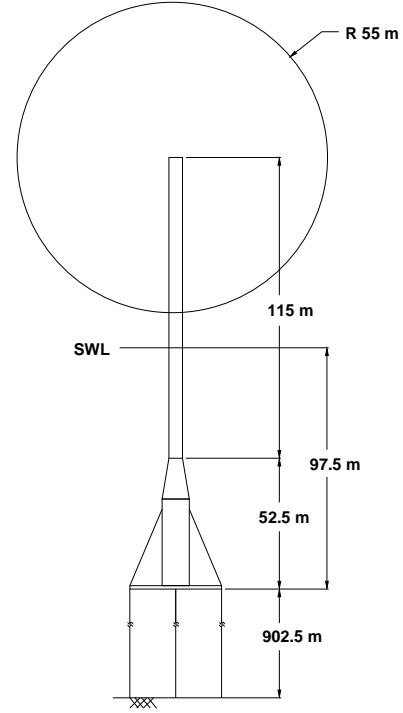


Figure 4: Example turbine tower

The thrust force for wind perpendicular to the swept area of the blades is approximately (e.g., [6]):

$$F_b = \frac{1}{2} C_T \rho_a A_b V_{rb}^2 \quad (45)$$

where ρ_a is the density of air; A_b is the swept area of the blades; C_T is the thrust coefficient. The force is in the direction of V_{rb} , the velocity of the wind relative to the RNA along the negative B -axis.

Wave loads are estimated using the well-known Morison equation in the (X, Y, Z) system (e.g., [12]):

$$\vec{f}_n = C_m \rho \frac{\pi}{4} D^2 \dot{\vec{V}}_n - C_a \rho \frac{\pi}{4} D^2 \dot{\vec{V}}_t + \frac{1}{2} \rho C_d D \vec{V}_{rt} |\vec{V}_{rt}| \quad (46)$$

where ρ is the density of sea water; D is the diameter of the tower; C_m is the inertia coefficient; C_a is the added mass coefficient, and C_d is the drag coefficient. All velocities, accelerations and forces are normal to the central axis of the tower: \vec{f}_n is the wave force per unit length of the tower (Fig. 3). The kinematic acceleration normal to the axis of the tower is $\dot{\vec{V}}_n$. The second acceleration term, which includes the tower acceleration $\dot{\vec{V}}_t$, is technically a force resulting from a hydrodynamic pressure, but this term effectively has been moved to the inertial side of the equation as

the basis for calculation of added mass. Added mass is included in the calculation of the center of mass and moment of inertia of the body, and so should not be included here. The result is that the relative velocity, \vec{V}_{rt} , is applied in the Morison drag term, but the absolute acceleration, \vec{V}_n , is applied in the acceleration term. For a symmetrical tower, wave forces resulting from Eqn. (46) are independent of θ_3 , but velocities in the θ_3 -direction do introduce meaningful damping. Damping in the θ_3 -direction can be added directly to the L.H.S. of Eqn. (14) as $C_z \dot{\theta}_3 |\dot{\theta}_3|$.

8.1 Case 1 - Free vibration: Fig. 5 shows a time-history of tower motions. Euler angle θ_1 corresponds to centerline of the tower leaning away from the vertical Z -axis, and θ_2 indicates the angle of revolution around the Z -axis. Angle θ_1 cannot change sign: jumps of π radians in θ_2 correspond to the tower passing through a vertical position. The monotonic increase in θ_2 indicates continuous tower revolution around the vertical Z -axis. The third Euler angle, η , is also shown. The divergence between η and θ_2 is reasonable since the twist of the mooring system must have a zero mean and $\dot{\theta}_Z = \dot{\theta}_2 + \dot{\eta} \cos \theta_1$ (Eqn. 15).

Finally, Fig. 5 does not show any change in energy as the process progresses in time, which is appropriate for undamped free vibration. Much longer simulations have also been observed to conserve system energy.

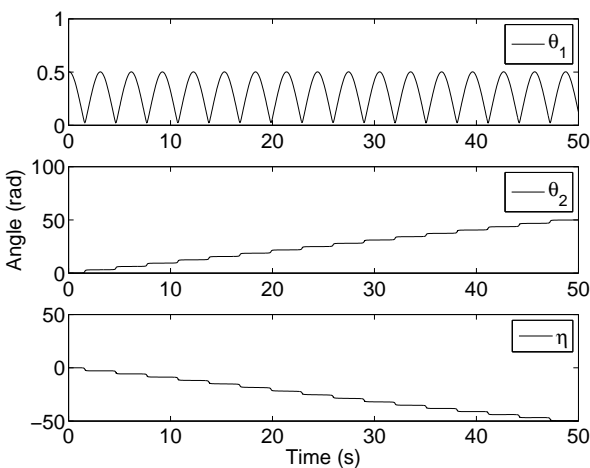


Figure 5: Case 1: Free Vibration

8.2 Case 2 - 3-D angular motion with steady wind and regular waves: Figs. 6–8 show time-histories resulting from simulation including wind and wave forcing, using the full 3-D equations

of motion. Aerodynamic and hydrodynamic damping are implicitly included in the θ_1 and θ_2 directions, and viscous damping is applied to the θ_3 direction. The figures show angular motions induced by the initial conditions of the simulation die out relatively quickly. There is an apparent phase-coupling between the three Euler angles in Fig. 6, but self-rotation of the tower in space, θ_3 , which is a combination of θ_1 , θ_2 and η , does not appear to be phase-linked to these Euler angles. After about $t = 40$ sec, the θ_2 motion has alternating positive and negative jumps; these jumps, which occur at minimum θ_1 , indicate the tower is moving back and forth across the direction of the wind. Fig. 7 shows the self-rotation of the tower about the z -axis, which has a non-zero mean; self-rotation is not equivalent to rotation at the mooring system, θ_Z , because the z -axis is moving in space. Fig. 8 shows the nutation of the RNA. The wind force causes θ to have mean slightly less than the $-\pi/2$ (-1.57 radians) of a vertical tower. The longer 1,000 second simulation time also shows that after the initial transients die-out the dynamic behavior does remain reasonably steady.

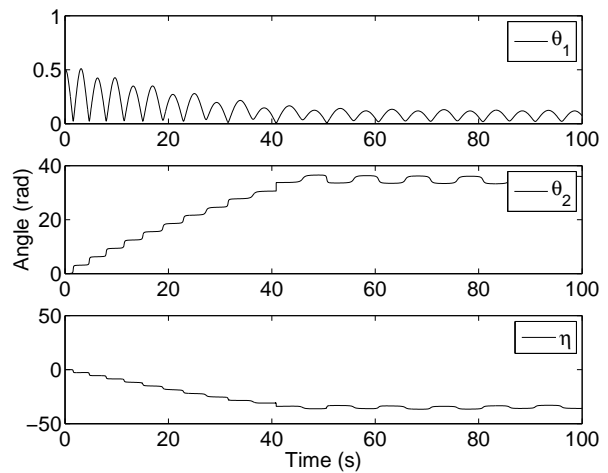


Figure 6: Case 2: Motions due to wind and waves

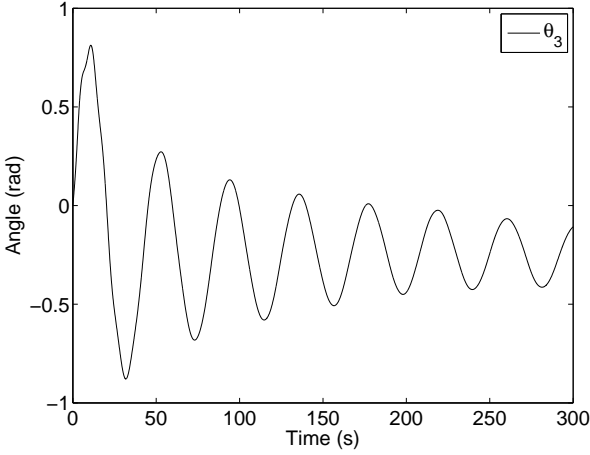


Figure 7: Case 2: Self-rotation of the tower

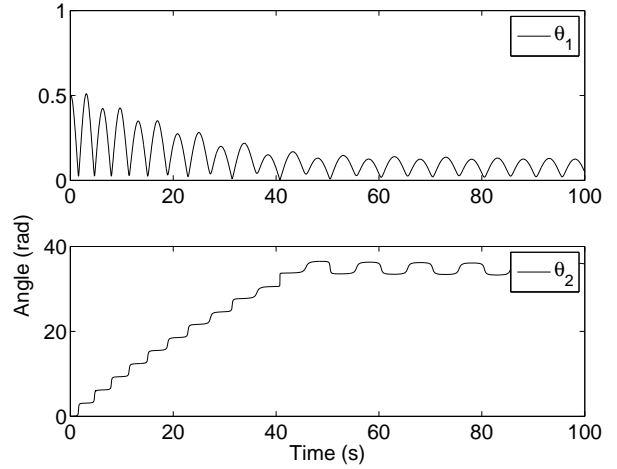


Figure 9: Case 3: Angular motions computed using 2-D Equations of Motion

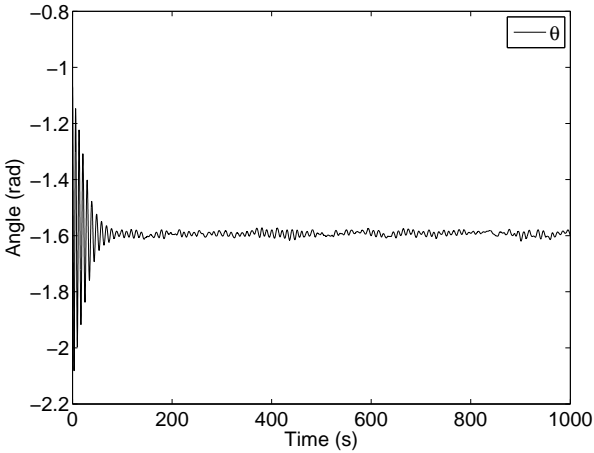


Figure 8: Case 2: Nutation of the RNA

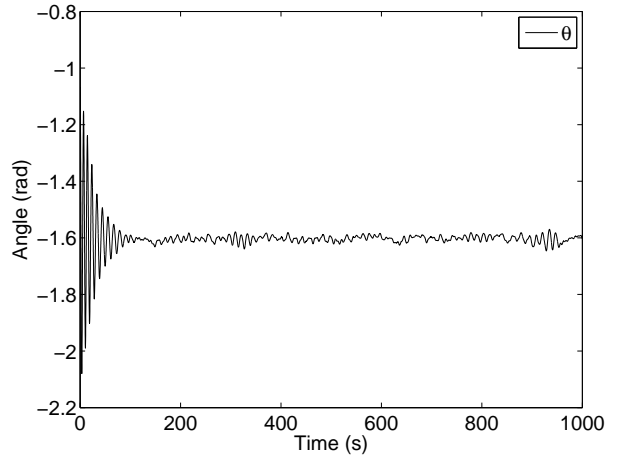


Figure 10: Case 3: Nutation of the RNA computed using 2-D Equations of Motion

8.3 Case 3 - Reduction to 2 Degrees of Freedom: Figs. 9 and 10 show time-histories resulting from simulation of a forced vibration case being solved using the simplified 2-D Euler equations of motion (Eqns. (21)-(22)). The forcing, damping and initial conditions are the same as in Case 2. Comparing Figs. 6 and 9, it is apparent that the general behavior and magnitude of the tower motion is well predicted using only two degrees of freedom, though there is a slight change in the θ_1 and θ_2 response frequencies (23 peaks in Fig. 6 vs 22 in Fig. 9). Comparing Figs. 8 and 10, however, shows that prediction of the nutation angle is compromised by the simplified method in both magnitude and frequency. This discrepancy results from the fact that nutation, θ , is linked to the relationship between ϕ and θ_2 , and ϕ is closely related to the θ_3 motion of the tower, which is not computed as part of the simplified procedure.

9. Conclusions: A set of 3-1-3 sequence Euler angles is introduced to describe the rigid-body motion of a floating wind turbine as a single rigid body, without consideration of nacelle yaw or blade spin (Fig. 1). Euler's equations of motion are analytically derived (Eqns. (9)-(11)) for numerical solution in the time-domain. Transformations between the non-rotating (X, Y, Z) and rotating (x, y, z) coordinate systems are developed in terms of Euler angles for the rigid body (Eqn. (36)) such that motions and environmental forcing can be transformed at each time step. The procedure enables time-domain simulations to include full coupling between the external moments and the motion of the body. A simplified version of the Euler equations of motion is also de-

veloped in which the rotation of the tower about its own centerline is neglected (Eqns. (21)–(22)).

An example shows simulation results from a MATLAB implementation of the complete 3-D Euler dynamics equations and also of the simplified 2-D version. A free vibration case of complete 3-D version demonstrates the effectiveness of the Euler dynamics equations. Two forced-vibration cases are also presented to compare results of the 3-D and 2-D versions of the solution. Both the complete Euler equations of motion and its simplified version offer similar θ_1 and θ_2 motions, which dominate the dynamic behavior of the system. More recent work builds upon this one free body diagram dynamic model to consider the RNA and tower as separate bodies, enabling quantification of the important dynamic effects of nacelle yaw and rotor spin. Ongoing work in this area is to reformulate and expand the overall methodology to the general motion of n rigid bodies. The generalized solution may be relevant to a broad variety of rotating machinery subject to angular acceleration.

10. Acknowledgements: This work was supported by the National Science Foundation, Division of Civil and Mechanical Systems under Agreement Number CMS-0448730. Any opinions, findings, and conclusions or recommendations expressed in this material are those of the authors and do not necessarily reflect the view of the National Science Foundation.

11. Nomenclature:

(X, Y, Z) : Translating coordinate system with respect to the earth, with the origin O fixed at the center of mass of the tower

(x, y, z) : Rotating coordinate system with the origin O fixed at the center of mass of the tower; the z -axis is fixed on the centerline of the tower while the x - and y -axes rotate about the z -axis independent of body rotations about that axis.

(X_n, Y_n, Z_n) : Translating coordinate system with respect to the earth, with the origin O' fixed at the center of mass of the RNA

(A, B, C) : Rotating coordinate system with the origin O' fixed at the center of mass of the RNA

B -axis: Spinning axis of the blades

B_p -axis: Horizontal projection of the B -axis on the XOY plane

y_p -axis: Horizontal projection of the y -axis on the XOY plane

$(\theta_1, \theta_2, \eta)$: Three 3-1-3 sequence Euler angles used to describe the rotation of the tower, where θ_1 is measured from the Z -axis to the z -axis with the positive direction along the x -axis; θ_2 is measured from the X -axis to the x -axis with the positive direction along the Z -axis; η is the rotation along the z -axis with the positive direction along the z -axis.

θ_3 : Physical self-rotation of the tower in the space with the positive direction along the z -axis

(ϕ, θ, ψ) : Three 3-1-3 sequence Euler angles used to describe the rotation of the RNA, also called precession, nutation and spin angles, where ϕ is measured from the Y -axis to the B_p -axis with the positive direction along the Z -axis; θ is measured from the Z -axis to the B -axis with the positive direction along the C -axis; ψ is the spinning around the B -axis with the positive direction along the B -axis.

λ : Measured from the B_p -axis to the B -axis with the positive direction along the C -axis

α : Measured from the y_p -axis to the B_p -axis with the positive direction along the Z -axis

C_T : Thrust coefficient, used to calculate the wind forces on the blades swept area

References:

- [1] J. M. Longuski, "Real solutions for the attitude motion of a self-excited rigid body," the 41st Congress of the International Astronautical Federation, 1990.
- [2] M. T. U. Mulk and J. Falzarano, "Complete six-degrees-of-freedom nonlinear ship rolling motion," *Journal of Offshore Mechanics and Arctic Engineering*, vol. 116, no. 4, pp. 191–201, 1994.
- [3] J. M. Jonkman and L. B. J. Marshal, "Fast user's guide," Tech. Rep. NREL/EL-500-38230, National Renewable Energy Laboratory, 2005.
- [4] C. H. Lee, *WAMIT Theory Manual*. Dept. of Ocean Engineering, M.I.T., 1995.

- [5] J. Jonkman, "Dynamic modeling and loads analysis of an offshore floating wind turbine," Tech. Rep. NREL/TP-500-41958, NREL National Energy Renewal Laboratory, 2007.
- [6] F. G. Nielsen, "Integrated dynamic analysis of floating offshore wind turbines," Proceedings of the 25th International Conference on Offshore Mechanics and Arctic Engineering, 2006.
- [7] S. Shim and M. H. Kim, "Rotor-floater-tether coupled dynamic analysis of offshore floating wind turbines," Proceedings of the Eighteenth International Offshore and Polar Engineering Conference, 2008.
- [8] R. C. Hibbeler, *Engineering Mechanics - Statics and Dynamics*. Pearson Prentice Hall, 2004.
- [9] D. Eberly, "Euler angle formulas," Tech. Rep. <http://www.geometrictools.com/>, Geometric Tools, LLC, 2008.
- [10] T. Krogh, "HAWC load simulation of generic 5mw offshore wind turbine model," tech. rep., Riso National Laboratory, 2004.
- [11] J. P. Jackson, S. C. Bush, and S. D. Copeland, "Ultra-deepwater floating windmills," tech. rep., Undergraduate Capstone Design Project, MASE-407, Texas A&M University, 2006.
- [12] T. Sarpkaya and M. Issacson, *Mechanics of Wave Forces on Offshore Structures*. Van Nostrand Reinhold Company, 1981.